1 A Particle–Partition of Unity Method Part V: Boundary Conditions

Michael Griebel[1] and Marc Alexander Schweitzer[1]

Sonderforschungsbereich 256 Nonlinear Partial Differential Equations, Institut für Angewandte Mathematik, Universität Bonn, Wegelerstr. 6, D-53115 Bonn, Germany.

Abstract In this sequel to [12, 13, 14, 15] we focus on the implementation of Dirichlet boundary conditions in our partition of unity method. The treatment of essential boundary conditions with meshfree Galerkin methods is not an easy task due to the non-interpolatory character of the shape functions. Here, the use of an almost forgotten method due to Nitsche from the 1970's allows us to overcome these problems at virtually no extra computational costs. The method is applicable to general point distributions and leads to positive definite linear systems. The results of our numerical experiments, where we consider discretizations with several million degrees of freedom in two and three dimensions, clearly show that we achieve the optimal convergence rates for regular and singular solutions with the (adaptive) h-version and (augmented) p-version.

Key words: meshfree methods, meshless methods, partition of unity method, Galerkin method, h-version, p-version

1.1 Introduction

Meshfree methods for the numerical treatment of partial differential equations gained much attention in recent years. These methods allow for the construction of shape functions without the need of a mesh or grid so that they are promising approaches to overcome the problem of mesh generation.

Since meshfree methods are independent of a mesh, their shape functions are in general more complex than finite element shape functions. In a meshfree method the shape functions are usually piecewise rational functions, whereas in a finite element method (FEM) they are piecewise polynomials. This makes the meshfree Galerkin discretization of a partial differential equation (PDE) more challenging than its discretization with a FEM. See [12, 13, 27, 28] for details on the discretization process with the partition of unity method (PUM). Furthermore, the shape functions are in general non-interpolatory which makes the design of optimal linear solvers [14] as well as the implementation of essential boundary conditions not an easy task.

Many different approaches toward the treatment of Dirichlet problems have been proposed over the years [4, 10, 12, 13, 16, 17, 19, 22, 27]. Most of them, however, suffer from one or several drawbacks (restrictions on the distribution of the discretization points, need for an additional boundary function space, saddle-point structure, non-optimal convergence rates, etc.). Yet,

the problem was in fact already solved in the early 1970's when Nitsche [23] developed a general approach for the treatment of essential boundary conditions where the trial and test functions do not have to fulfill the boundary conditions. Nitsche's method, however, seems to be quite unknown. Recently, Stenberg [29] revived the interest in this non-standard method by showing its connection to some stabilization techniques for the Lagrange multiplier method.

In this paper we present the implementation of essential boundary conditions by Nitsche's method in the context of our partition of unity method for the numerical solution of elliptic PDE. The remainder of the paper is organized as follows. We begin with a short review of the construction of PUM spaces, the Galerkin discretization of an elliptic PDE and the multilevel solution of the arising linear block-system in §1.2. The treatment of essential boundary conditions is presented in §1.3. Here, we discuss the various approaches and their difficulties and give a detailed introduction to Nitsche's method. Then, we present the results of our numerical experiments where we apply our PUM Dirichlet problems with regular and singular solutions in two and three dimensions in §1.4. Finally, we conclude with some remarks in §1.5.

1.2 Partition of Unity Method

In the following, we shortly review the construction partition of unity spaces and the meshfree Galerkin discretization of an elliptic PDE, see [12, 13] for details. Furthermore, we give a summary of the efficient multilevel solution of the arising linear block-system, see [14] for details.

1.2.1 Construction of Partition of Unity Method

In a partition of unity method, we define a global approximation u^{PU} simply as a weighted sum of local approximations u_i,

$$u^{\mathrm{PU}}(x) := \sum_{i=1}^{N} \varphi_i(x) u_i(x). \tag{1.1}$$

These local approximations u_i are completely independent of each other, i.e., the local supports $\omega_i := \mathrm{supp}(u_i)$, the local basis $\{\psi_i^n\}$ and the order of approximation p_i for every single $u_i := \sum u_i^n \psi_i^n \in V_i^{p_i}$ can be chosen independently of all other u_j. Here, the functions φ_i form a partition of unity (PU). They are used to splice the local approximations u_i together in such a way that the global approximation u^{PU} benefits from the local approximation orders p_i yet it still fulfills global regularity conditions, see [12]. Hence, the global approximation space on Ω is defined as

$$V^{\mathrm{PU}} := \sum_i \varphi_i V_i^{p_i} = \sum_i \varphi_i \operatorname{span}\langle\{\psi_i^n\}\rangle = \operatorname{span}\langle\{\varphi_i\psi_i^n\}\rangle. \tag{1.2}$$

The starting point for any meshfree method is a collection of N independent points $P := \{x_i \in \mathbb{R}^d \,|\, x_i \in \overline{\Omega}, i = 1, \ldots, N\}$. In the PU approach we need to construct a partition of unity $\{\varphi_i\}$ on the domain of interest Ω to define an approximate solution (1.1) where the union of the supports $\operatorname{supp}(\varphi_i) = \overline{\omega_i}$ covers the domain $\overline{\Omega} \subset \bigcup_{i=1}^N \omega_i$ and $u_i \in V_i^{p_i}(\omega_i)$ is some locally defined approximation of order p_i to u on ω_i. Thus, the first (and most crucial) step in a PUM is the efficient construction of an appropriate cover C_Ω. This is not and easy task [13, 27]. Throughout this paper we use a tree-based construction algorithm for d-rectangular covers presented in [13]. Here, the cover patches ω_i are products of intervals $(x_i^l - h_i^l, x_i^l + h_i^l)$. With the help of weight functions W_k defined on these cover patches ω_i we can easily generate a partition of unity by *Shepard's method*, i.e., we define

$$\varphi_i(x) = \frac{W_i(x)}{\sum_{\omega_k \in C_\Omega^i} W_k(x)}, \tag{1.3}$$

where $C_i := \{\omega_j \in C_\Omega \,|\, \omega_i \cap \omega_j \neq \emptyset\}$ is the set of all geometric neighbors of a cover patch ω_i. Due to the use of d-rectangular patches ω_i, the most natural choice for a weight function W_i is a product of one-dimensional functions, i.e., $W_i(x) = \prod_{l=1}^d W_i^l(x^l) = \prod_{l=1}^d \mathcal{W}\left(\frac{x - x_i^l + h_i^l}{2h_i^l}\right)$ with $\operatorname{supp}(\mathcal{W}) = [0, 1]$ such that $\operatorname{supp}(W_i) = \overline{\omega_i}$. It is sufficient for this construction to choose a one-dimensional weight function $\mathcal{W}$ with the desired regularity which is non-negative. The partition of unity functions φ_i inherit the regularity of the generating weight function $\mathcal{W}$. We always use a normed B-spline [27] as the generating weight function $\mathcal{W}$.

In general, a partition of unity $\{\varphi_i\}$ can of course only recover the constant function on the domain Ω. Hence, we need to improve the approximation quality to use the method for the discretization of a PDE. To this end, we multiply the partition of unity functions φ_i locally with polynomials ψ_i^n. Since we use d-rectangular patches ω_i only, a local tensor product space is the most natural choice. Throughout this paper, we use products of univariate Legendre polynomials as local approximation spaces $V_i^{p_i}$, i.e., we choose

$$V_i^{p_i} = \operatorname{span}\langle\{\psi_i^n \,|\, \psi_i^n = \prod_{l=1}^d \mathcal{L}_i^{\hat{n}_l}, \|\hat{n}\|_1 = \sum_{l=1}^d \hat{n}_l \leq p_i\}\rangle,$$

where $\hat{n}$ is the multi-index of the polynomial degrees $\hat{n}_l$ of the univariate Legendre polynomials $\mathcal{L}_i^{\hat{n}_l} : [x_i^l - h_i^l, x_i^l + h_i^l] \to \mathbb{R}$, and n is the index associated with the product function $\psi_i^n = \prod_{l=1}^d \mathcal{L}_i^{\hat{n}_l}$.

In summary, we can view the construction given above as follows

$$\begin{pmatrix} \{x_i\} \\ \mathcal{W} \\ \{p_i\} \end{pmatrix} \to \begin{pmatrix} \{\omega_i\} \\ \{W_i\} \\ \{V_i^{p_i} = \operatorname{span}\langle\psi_i^n\rangle\} \end{pmatrix} \to \begin{pmatrix} \{\varphi_i\} \\ \{V_i^{p_i}\} \end{pmatrix} \to V^{\mathrm{PU}} = \sum \varphi_i V_i^{p_i},$$

where the set of points $P = \{x_i\}$, the generating weight function $\mathcal{W}$ and the local approximation orders p_i are assumed to be given.

1.2.2 Basic Convergence Theory

In this section we state the notation and basic theory of the partition of unity method as developed by Babuška and Melenk in [5, 6]. Crucial to the theory of the partition of unity method is the notion of a (M, C_∞, C_∇) partition of unity. The conditions formulated in the following definitions allow to show the basic approximation properties as given in Theorem 1 of a partition of unity space V^{PU} (1.2).

Definition 1 (Partition of Unity). *Let $\Omega \subset \mathbb{R}^d$ be an open set, let $C_\Omega = \{\omega_i\}$ be an open cover of Ω satisfying a point-wise overlap condition*

$$\exists M \in \mathbb{N} \quad \forall x \in \Omega \quad \mathrm{card}(\{i \,|\, x \in \omega_i\}) \leq M\,.$$

Let $\{\varphi_i\}$ be a Lipschitz partition of unity subordinate to the cover C_Ω satisfying

$$\begin{aligned} \mathrm{supp}(\varphi_i) \subset \overline{\omega_i} \quad &\text{for all } i, & \textstyle\sum_i \varphi_i \equiv 1 \ &\text{on } \Omega, \\ \|\varphi_i\|_{L^\infty(\mathbb{R}^d)} \leq C_\infty, & & \|\nabla\varphi_i\|_{L^\infty(\mathbb{R}^d)} &\leq \tfrac{C_\nabla}{\mathrm{diam}(\omega_i)}, \end{aligned}$$

where C_∞ and C_∇ are two positive constants. Then $\{\varphi_i\}$ is called a (M, C_∞, C_∇) partition of unity subordinate to the cover C_Ω. The partition of unity is said to be of degree $k \in \mathbb{N}_0$ if $\varphi_i \in \mathcal{C}^k(\mathbb{R}^d)$ for all i. The covering sets ω_i are called patches.

Definition 2 (Partition of Unity Space). *Let $C_\Omega = \{\omega_i\}$ be an open cover of $\Omega \subset \mathbb{R}^d$ and let $\{\varphi_i\}$ be a (M, C_∞, C_∇) partition of unity subordinate to C_Ω. Let $V_i^{p_i} = \mathrm{span}\langle\{\psi_i^n\}\rangle \subset H^1(\Omega \cap \omega_i)$ be given. Then the space*

$$V^{\mathrm{PU}} := \sum_i \varphi_i V_i^{p_i} = \sum_i \varphi_i \,\mathrm{span}\langle\{\psi_i^n\}\rangle = \mathrm{span}\langle\{\varphi_i\psi_i^n\}\rangle$$

is called a partition of unity space. The space V^{PU} is said to be of degree $k \in \mathbb{N}$ if $V^{\mathrm{PU}} \subset \mathcal{C}^k(\Omega)$. The spaces $V_i^{p_i}$ are referred to as the local approximation spaces.

Theorem 1 (Approximation Property). *Let $\Omega \subset \mathbb{R}^d$ be given. Let $C_\Omega = \{\omega_i\}$, $\{\varphi_i\}$ and $V_i^{p_i}$ be as in Definitions 1 and 2. Let $u \in H^1(\Omega)$ be the function to be approximated. Assume that the local approximation spaces $V_i^{p_i}$ have the following approximation properties: On each patch $\Omega \cap \omega_i$, the function u can be approximated by a function $v_i \in V_i^{p_i}$ such that $\|u - v_i\|_{L^2(\Omega\cap\omega_i)} \leq \hat{\epsilon}_i$, and $\|\nabla(u - v_i)\|_{L^2(\Omega\cap\omega_i)} \leq \tilde{\epsilon}_i$ hold. Then the function*

$$u^{\mathrm{PU}} := \sum_i \varphi_i v_i \in V \subset H^1(\Omega)$$

satisfies

$$\|u - u^{\mathrm{PU}}\|_{L^2(\Omega)} \leq \sqrt{M} C_\infty \Big(\sum_{i=1}^{N} \hat{\epsilon}_i^2 \Big)^{\frac{1}{2}},$$
$$\|\nabla(u - u^{\mathrm{PU}})\|_{L^2(\Omega)} \leq \sqrt{2M} \Big(\sum_{i=1}^{N} \big(\frac{C_\nabla}{\mathrm{diam}(\omega_i)} \big)^2 \hat{\epsilon}_i^2 + C_\infty^2 \tilde{\epsilon}_i^2 \Big)^{\frac{1}{2}}.$$

Proof. See [5, 6].

Due to this theorem we can use the partition of unity method as an h-version, a p-version or even an hp-version. From the above estimate we can see that the approximation property of the approximation space V^{PU} may be improved via the reduction of the diameters of the cover patches ω_i (the insertion of points x_i) or via the enhancement of the approximation qualities of the local spaces $V_i^{p_i}$ (the increment of the local approximation order p_i). These refinement strategies are independent of each other, thus we may use both at the same time. Since the PUM only employs a scattered data set, an adaptive h-refinement (by the insertion of new points x_i) does not have to cope with problems caused by the grid-structure like hanging nodes, etc. Furthermore, there are no compatibility restrictions on the local spaces $V_i^{p_i}$. Hence, we may also employ an adaptive p-refinement on the local spaces $V_i^{p_i}$, i.e., we may use a different order of approximation p_i and even different basis functions ψ_i^n in different parts of the domain.

1.2.3 Galerkin Discretization of Elliptic Equations

We want to solve elliptic boundary value problems of the type

$$\begin{aligned} Lu &= f \text{ in } \Omega \subset \mathbb{R}^d, \\ Bu &= g \text{ on } \partial\Omega, \end{aligned} \tag{1.4}$$

where L is a symmetric partial differential operator of second order and B expresses suitable boundary conditions.

In the following let $a(\cdot,\cdot)$ be the continuous and elliptic bilinear form induced by L on $V := H^1(\Omega)$. We discretize the partial differential equation using Galerkin's method. Then, we have to compute the stiffness matrix

$$A = (A_{(i,n),(j,m)}), \text{ with } A_{(i,n),(j,m)} = a(\varphi_j \psi_j^m, \varphi_i \psi_i^n) \in \mathbb{R},$$

and the right hand side vector

$$\hat{f} = (f_{(i,n)}), \text{ with } f_{(i,n)} = \langle f, \varphi_i \psi_i^n \rangle_{L^2} = \int_\Omega f \varphi_i \psi_i^n \in \mathbb{R}.$$

If we restrict ourselves for reasons of simplicity to the case $L = -\Delta$ we have to compute the integrals $\int_\Omega \varphi_i \psi_i^n f$ for the right hand side and the integrals

$\int_\Omega \nabla(\varphi_i\psi_i^n)\nabla(\varphi_j\psi_j^m)$ for the stiffness matrix. Recall that φ_i is defined by (1.3), i.e.

$$\varphi_i(x) = \frac{W_i(x)}{\sum W_k(x)}.$$

Now we carry out the differentiation in $\int_\Omega \nabla(\varphi_i\psi_i^n)\nabla(\varphi_j\psi_j^m)$. With the notation $\mathcal{S} := \sum W_k$, $\mathcal{T} := \sum \nabla W_k$ and $\mathcal{G}_i := \nabla W_i \mathcal{S} - W_i \mathcal{T}$ we end up with the integrals

$$\begin{aligned} a(\varphi_j\psi_j^m, \varphi_i\psi_i^n) = &\int_\Omega \mathcal{S}^{-4}\mathcal{G}_i\psi_i^n\mathcal{G}_j\psi_j^m \quad + \int_\Omega \mathcal{S}^{-2}W_i\nabla\psi_i^n W_j\nabla\psi_j^m + \\ &\int_\Omega \mathcal{S}^{-3}\mathcal{G}_i\psi_i^n W_j\nabla\psi_j^m + \int_\Omega \mathcal{S}^{-3}W_i\nabla\psi_i^n\mathcal{G}_j\psi_j^m \end{aligned} \tag{1.5}$$

for the stiffness matrix and the integrals

$$\langle f, \varphi_i\psi_i^n\rangle_{L^2} = \int_\Omega \mathcal{S}^{-1}W_i\psi_i^n f \tag{1.6}$$

for the right hand side. These integrands may have quite a number of jumps of significant size since we use piecewise polynomial weights W_i whose supports ω_i overlap in the Shepard construction (1.3). Therefore, the integrals of the weak form have to be computed with certain care using an appropriate numerical quadrature scheme, see [12, 13].

1.2.4 Multilevel Solution of Resulting Linear System

The product structure of the shape functions $\varphi_i\psi_i^n$ implies two natural block-partitions of the resulting linear system $A\tilde{u} = \hat{f}$, where $\tilde{u}$ denotes a coefficient vector and $\hat{f}$ denotes a moment vector.

1. The stiffness matrix A can be arranged in *spatial blocks*. A spatial block A_{nm} corresponds to a discretization of the PDE on the complete domain Ω using the trial functions $\varphi_j\psi_j^m$ and the test function $\varphi_i\psi_i^n$ with fixed n and m. Here, all blocks A_{nm} are sparse matrices and have the same row and column dimensions which corresponds to the number of partition of unity functions φ_i.
2. The stiffness matrix A may also be arranged in *polynomial blocks*. Here, a single block A_{ij} corresponds to a local discretization of the PDE on the domain $\omega_i \cap \omega_j \cap \Omega$. The polynomial blocks A_{ij} are dense matrices and may have different dimensions corresponding to the dimensions of the local approximation spaces $V_j^{p_j}$ and $V_i^{p_i}$.

This separation of the degrees of freedom into local approximation functions ψ_i^n and partition of unity functions φ_i can be used to define two different multilevel concepts [14]. Throughout this paper we assume that the stiffness matrix is given in polynomial block-form and we use the corresponding spatial multilevel solver developed in [14] for the fast and efficient solution of

the resulting large sparse linear block-system $A\tilde{u} = \hat{f}$, where $\tilde{u}$ denotes a coefficient block-vector and $\hat{f}$ a moment block-vector.

In a multilevel method we need a sequence of discretization spaces V_k with $k = 0, \ldots, J$ where J denotes the finest level. To this end we construct a sequence of PUM spaces V_k^{PU} as follows. We use a tree-based algorithm developed in [13, 14] to generate a sequence of point sets P_k and covers C_Ω^k from a given initial point set $\tilde{P}$. Following the construction given in §1.2.1 we can then define an associated sequence of PUM spaces V_k^{PU}. Note that these spaces are nonnested, i.e., $V_{k-1}^{\mathrm{PU}} \not\subset V_k^{\mathrm{PU}}$, and that the shape functions $\varphi_{i,k}\psi_{i,k}^n$ are non-interpolatory. Thus, we need to construct appropriate transfer operators $I_{k-1}^k : V_{k-1}^{\mathrm{PU}} \to V_k^{\mathrm{PU}}$ and $I_k^{k-1} : V_k^{\mathrm{PU}} \to V_{k-1}^{\mathrm{PU}}$. With such transfer operators I_{k-1}^k, I_k^{k-1} and the stiffness matrices A_k coming from the Galerkin discretization on each level k we can then set up a standard multiplicative multilevel iteration to solve the linear system $A_J\tilde{u}_J = \hat{f}_J$.

Our multilevel solver utilizes special localized L^2-projections for the interlevel transfers and a block-smoother to treat all local degrees of freedom ψ_i^n within a patch ω_i simultaneously. The convergence rates of this multilevel iteration are independent of the number of cover patches $\mathrm{card}(C_\Omega^J)$ and only slightly dependent on the polynomial degrees. The typical convergence rate of a $V(1,1)$-cycle is $\rho \leq 0.25$ for a PUM space with linear local approximation spaces. For further details see [14].

1.3 Boundary Conditions

Our PUM shape functions $\varphi_i\psi_i^n$ are non-interpolatory since the partition of unity functions φ_i are (in general) non-interpolatory, i.e., $\varphi_i(x_j) \neq \delta_{ij}$. Furthermore the usage of local approximation spaces $V_i^{p_i}$ with $\dim(V_i^{p_i}) > 1$ generates an approximation space $V^{\mathrm{PU}} = \sum_i \varphi_i V_i^{p_i}$ with more degrees of freedom than interpolation nodes x_i. Thus, we have to cope with the problem: How to fulfill boundary conditions?

First consider (1.4) with Neumann boundary conditions $Bu = u_n := \partial u/\partial n := \nabla u \cdot n = g$ on $\partial\Omega$, where n denotes the outer normal. Here, we learn from the variational formulation

$$F(v) := \frac{1}{2}a(v,v) - \langle f, v\rangle_{L^2} - \int_{\partial\Omega} gv \to \min\{v \in H^1(\Omega)\}, \tag{1.7}$$

that the trial functions v have to fulfill no additional constraint besides being from the definition space $H^1(\Omega)$ of the differential operator L in its weak form. The boundary conditions are not imposed explicitly on the function space. Thus, the basis of a finite-dimensional subspace $V \subset H^1(\Omega)$ used to approximate the solution of (1.7) may be compiled of arbitrary functions $v \in H^1(\Omega)$. The basis functions do not need to be interpolatory. Hence, we may use our functions $\varphi_i\psi_i^k$ as trial and test functions in a Galerkin procedure without any modification.

However, Dirichlet boundary conditions $Bu = u = g$ on $\partial\Omega$ explicitly impose the values of the solution u on the boundary $\partial\Omega$. Thus, the trial space of the usual weak formulation

$$\text{Find } u \in H^1_g(\Omega): \quad a(u,v) = \langle f, v\rangle_{L^2} \text{ for all } v \in H^1_0(\Omega)$$

is not the complete space $H^1(\Omega)$ but $H^1_g(\Omega) := \{v \in H^1(\Omega) \,|\, u = g \text{ on } \partial\Omega\}$, whereas the test space is $H^1_0(\Omega)$. Note that we can enforce vanishing Dirichlet boundary conditions within the PUM by the selection of appropriate local approximation spaces $V_i^{p_i}$, i.e., we need $\psi_i^k|_{\partial\Omega} \equiv 0$ for all local basis functions ψ_i^k [4, 10]. But the implementation of a trial space $V \subset H^1_g(\Omega)$ with $g \not\equiv 0$ by the selection of appropriate local approximation spaces is not feasible.

There are many different approaches toward the treatment of Dirichlet boundary conditions with meshfree methods [4, 10, 16, 27], e.g.

1. coupling to mesh-based methods close to the boundary [19],
2. penalty or perturbation methods [17, 22],
3. the Lagrange multiplier method [12, 27],
4. and Nitsche's method [4, 28].

Obviously the coupling of a meshfree method to a mesh-based method destroys the meshfree character of the original method just for the sake of the implementation of Dirichlet boundary conditions. This loss of generality and freedom can hardly be justified. Furthermore, the coupling itself must be consistent with the local approximation orders p_i of the local spaces or we also experience an adverse effect on the approximation quality of the overall method only due to the poor implementation of Dirichlet boundary conditions.

The penalty or perturbation approaches are very general concepts for the implementation of constraints in a variational problem. In our setting we would introduce an additional surface term in the variational formulation to enforce the boundary conditions. This penalty term may change the properties of the functional and we need to be concerned with the issues of existence and uniqueness of a solution. Furthermore, we usually do not achieve the maximal rate of convergence [2, 4, 23], i.e., again we would experience a reduction in the approximation quality of the overall method just because of the inappropriate treatment of boundary conditions.

The Lagrange multiplier method is a general approach toward the solution of constrained minimization problems which is also used in the finite element [3, 8] and wavelet [20] context to implement essential boundary conditions. It is well-known that the method converges with the optimal rates if the function spaces involved, in our setting the interior PUM approximation space and the multiplier space on the boundary, fulfill a (discrete) Ladyzhenskaya–Babuška–Brezzi (or inf-sup) condition. Here, the main problem is the design of an appropriate multiplier space on the boundary. Within the finite element context Pitkäranta [24, 25, 26] showed that there is not much freedom in the

design of the multiplier space if the optimal convergence of the method is desired. Furthermore, the use of Lagrange multipliers (in general) leads to a saddle-point problem and the arising linear system is indefinite and the design of an optimal solver is not an easy task.

A different variational approach to Dirichlet problems due to Nitsche [23], however, allows for the use of subspaces $V_N \subset H^1(\Omega)$ which do not have to fulfill the boundary conditions explicitly, yet it gives the optimal rate of convergence. Let us consider the Poisson problem

$$\begin{aligned} -\Delta u &= f \text{ in } \Omega \subset \mathbb{R}^d, \\ u &= g \text{ on } \partial\Omega, \end{aligned} \tag{1.8}$$

for reasons of simplicity. We are interested in finding an approximate solution $u_N \in V_N \subset H^1(\Omega)$ to (1.8) — within optimal error bounds. In an early yet not widely known paper [23] Nitsche proposed to minimize the functional $J_N(v-u)$ among all $v \in V_N$ where u is the solution of (1.8),

$$J_N(w) := \int_\Omega |\nabla w|^2 - 2\int_{\partial\Omega} w w_n + \beta_N \int_{\partial\Omega} w^2,$$

and $\beta_N > 0$ depends only on the subspace V_N, i.e., the approximation u_N is given by $J(u_N - u) := \inf_{v\in V_N} J_N(v-u)$. Note that the subscript n denotes the normal derivative, i.e., $w_n = \nabla w \cdot n$, whereas the subscript N indicates a dependence on the discretization space $V_N \subset H^1(\Omega)$. The minimizer $u_N \in V_N$ can be computed from the input data f and g of (1.8) since

$$\begin{aligned} J_N(v-u) &= J_N(v) + J_N(u) - 2\left(\int_\Omega \nabla v \nabla u + \int_{\partial\Omega} u(\beta_N v - v_n) - v u_n\right), \\ &= J_N(v) + J_N(u) - 2\left(\int_\Omega f v + \int_{\partial\Omega} g(\beta_N v - v_n)\right). \end{aligned}$$

The corresponding weak formulation is given by $a_N(u_N, v) = \langle l_N, v\rangle$ for all $v \in V_N$ where

$$\begin{aligned} a_N(w,v) &:= \int_\Omega \nabla v \nabla w - \int_{\partial\Omega} v w_n - \int_{\partial\Omega} w v_n + \beta_N \int_{\partial\Omega} v w, \\ \langle l_N, v\rangle &:= \int_\Omega f v - \int_{\partial\Omega} g v_n + \beta_N \int_{\partial\Omega} g v. \end{aligned}$$

Although the bilinearform $a_N(\cdot,\cdot)$ is indefinite on the space $H^1(\Omega)$ it is symmetric positive definite on the subspace V_N under the assumptions that

$$\|v_n\|_{L^2(\partial\Omega)} \le C_N \|\nabla v\|_{L^2(\Omega)} \tag{1.9}$$

holds for all $v \in V_N$ with $C_N > 0$ and that $\beta_N > 2C_N^2$ since

$$\begin{aligned} a_N(v,v) &= \|\nabla v\|^2_{L^2(\Omega)} - 2\int_{\partial\Omega} v v_n + \beta_N \|v\|^2_{L^2(\partial\Omega)} \\ &\geq \|\nabla v\|^2_{L^2(\Omega)} - 2C_N \|v\|_{L^2(\partial\Omega)} \|\nabla v\|_{L^2(\Omega)} + \beta_N \|v\|^2_{L^2(\partial\Omega)} \\ &\geq \frac{1}{2}\|\nabla v\|^2_{L^2(\Omega)} + (\beta_N - 2C_N^2)\|v\|^2_{L^2(\partial\Omega)}. \end{aligned}$$

Nitsche furthermore proved optimal error estimates if the relation

$$C_N^2 \simeq \operatorname{diam}(\operatorname{supp}(\phi))^{-1} \tag{1.10}$$

for C_N in (1.9) holds for all basis functions $\phi \in V_N$ and if the respective approximation property is given in V_N. The proportionality (1.10) is valid e.g. if we have estimates of the form

$$\int_{\partial\Omega} |\phi_n|^2 \leq C_{N,1}(\operatorname{diam}(\operatorname{supp}(\phi)))^{d-1} \tag{1.11}$$

and

$$\int_{\Omega} |\nabla\phi|^2 \geq C_{N,2}(\operatorname{diam}(\operatorname{supp}(\phi)))^{d} \tag{1.12}$$

for all basis functions $\phi \in V_N$ with $\operatorname{supp}(\phi) \cap \partial\Omega \neq \emptyset$. Note that (1.11) and (1.12) essentially introduce some geometric constraints on the intersections $\operatorname{supp}(\phi) \cap \Omega$ and $\operatorname{supp}(\phi) \cap \partial\Omega$, i.e., in our meshfree context on the cover C_Ω or in the finite element context on the regularity of the mesh.

The proof of (1.10), i.e., of (1.11) and (1.12), for linear finite elements on a regular mesh is trivial since the first order derivatives $\partial_i\phi$ of a shape function ϕ are constant on an element. In general a proof of (1.10) is simplified when we only need to consider a regular reference configuration, i.e., where the map to the reference configuration is affine. Here, we find

$$\begin{aligned} \frac{\int_{\partial\,\operatorname{supp}(\phi)} |\phi_n|^2}{\int_{\operatorname{supp}(\phi)} |\nabla\phi|^2} &= \frac{\det(J_{\partial T}) \int_{\partial\omega_{\mathrm{ref}}} |\phi_n \circ \partial T|^2}{\det(J_T) \int_{\omega_{\mathrm{ref}}} |\nabla\phi \circ T|^2} \\ &= \frac{\det(J_{\partial T})}{\det(J_T)} C_{N,\mathrm{ref}} \\ &\simeq (\operatorname{diam}(\operatorname{supp}(\phi)))^{-1} C_{N,\mathrm{ref}} \end{aligned}$$

where $C_{N,\mathrm{ref}}$ is only dependent on the polynomial degree of the shape function ϕ. Thus, if we limit ourselves to the use of uniform covers and a fixed local approximation space we only need to consider very few reference cases (depending on the number of edges of $\operatorname{supp}(\varphi_i\psi_i^n) \cap \partial\Omega$ and the polynomial degree p_i of $V_i^{p_i}$). However, for the general situation where we have an irregular point distribution and locally varying approximation spaces this approach cannot be pursued. Furthermore, from a computational point of view we must

be interested in the *value* of C_N in (1.9), not only the type of the proportionality (1.10). Only a large enough value C_N will lead to a definite problem formulation. Yet, a wrong choice of the regularization parameter may have an impact on the condition number of the linear system or other adverse effects on the applicability of certain linear solvers. The parameter C_N is not only dependent on the support sizes but also on the selected local basis functions ψ_i^k for the space $V_i^{p_i}$ and the local approximation orders p_i. Hence, we need to be concerned with the automatic computation of a reliable estimate of C_N. Here, we decided to approach the estimate (1.9) as a generalized eigenvalue problem

$$\mathcal{A}x = \lambda \mathcal{B}x \tag{1.13}$$

where

$$\mathcal{A}_{(i,k),(j,m)} := \int_{\partial\Omega} (\varphi_j \psi_j^m)_n (\varphi_i \psi_i^k)_n$$

and

$$\mathcal{B}_{(i,k),(j,m)} := \int_{\Omega} \nabla(\varphi_j \psi_j^m) \nabla(\varphi_i \psi_i^k)$$

for all index pairs (i,k), (j,m) which correspond to a shape function which overlaps the boundary $\partial\Omega$, i.e., $\omega_i \cap \partial\Omega \neq \emptyset$ and $\omega_j \cap \partial\Omega \neq \emptyset$. Solving (1.13) for the maximal eigenvalue $\lambda_{\max}$ we get a good estimate for C_N^2.

Note that the assembly of the matrices $\mathcal{A}$ and $\mathcal{B}$ does not introduce a significant amount of additional computational costs. The entries of $\mathcal{B}$ are needed for the stiffness matrix anyway and can be re-used. The remaining additional costs associated with the computation of the regularization parameter β_N come from the solution of the eigenvalue problem (1.13). The eigenvalue $\lambda_{\max}$ can be computed very efficiently by a simultaneous Rayleigh-quotient minimization method [7, 11, 21] due to the similar structure of the matrices $\mathcal{A}$ and $\mathcal{B}$. Here, the minimization of $\frac{x^T \mathcal{B} x}{x^T \mathcal{A} x}$ only involves matrix-vector-products. We do not need to solve a linear system. Furthermore, the eigenvalue problem (1.13) involves only boundary degrees of freedom and is therefore of smaller dimension. Hence, the computational costs associated with the assembly of a Dirichlet problem are comparable to the costs associated with the respective Neumann problem.

Nitsche's method is closely related to some stabilized Lagrange multiplier techniques [29] which are used in Discontinuous Galerkin methods [1], Domain decomposition methods [9] and Mortar finite element methods [18, 30]. From our point of view, this approach provides the most natural implementation of Dirichlet boundary conditions for meshfree methods. The main advantages of Nitsche's method are:

1. It does *not* introduce constraints on the distribution of the points $x_i \in P$.
2. The problem formulation involves only the a single function space. There is no need of an additional appropriate function space on the boundary.
3. The method leads to symmetric definite linear systems. We do not need to be concerned with linear solvers for saddle-point problems.

Furthermore, we can automatically compute the regularization parameter β_N without significant extra computational costs. This is especially important for highly irregular point sets P, varying local basis functions ψ_i^k or varying local approximation orders p_i. Hence, we use Nitsche's method for the implementation of Dirichlet boundary conditions throughout this paper. In summary, the implementation of Neumann or Dirichlet boundary conditions involve only the evaluation of boundary integrals of the PUM shape functions $\varphi_i \psi_i^k$ and their gradients. We get the same rates of convergence for both types of boundary conditions and the arising linear systems are positive definite independent of the boundary conditions. The computational costs associated with the assembly of the stiffness matrix A and right-hand side vector $\hat{f}$ are comparable for both types of boundary conditions. Finally, we give the weak formulation of a Poisson problem

$$\begin{aligned} -\Delta u &= f \quad \text{in } \Omega \subset \mathbb{R}^d, \\ u &= g_D \text{ on } \Gamma_D \subset \partial\Omega, \\ u_n &= g_N \text{ on } \Gamma_N = \partial\Omega \setminus \Gamma_D, \end{aligned}$$

with mixed boundary conditions where the Dirichlet boundary conditions are realized with Nitsche's method and the Neumann boundary conditions are implemented in the standard fashion as an additional surface term on the right-hand side. This weak formulation

$$\int_\Omega \nabla u \nabla v + \int_{\Gamma_D} u(\beta v - v_n) - u_n v = \int_\Omega f v + \int_{\Gamma_D} g_D(\beta v - v_n) + \int_{\Gamma_N} g_N v,$$

where β now denotes the respective regularization parameter, is the problem formulation which we have implemented. Here, the volume and surface integrals are computed with the help of a sparse grid quadrature scheme presented in [13].

Note that the introduction of a space-dependent (i.e. level-dependent) regularization parameter may effect the quality of a multilevel solver for the resulting linear system. The regularization parameter grows with the number of levels due to the relation $\beta_l \sim h^{-1} = 2^l$ so that one approach could be the use of β_l from the finest level l also on the coarser levels $k < l$, i.e. $\beta_k = \beta := \beta_l$ for all $k = 0, \ldots, l$. With this choice for β we have the same variational form on all levels k. This approach, however, leads to an imbalance between the approximation of the boundary conditions and the approximation of the PDE in the domain on the different levels which may adversely effect the overall convergence rate of the multilevel solver. Furthermore, if we use the regularization from the finest level on all levels we need to fix the finest discretization level in advance. We cannot re-use the discretized systems from previous computations or levels if we need to refine the underlying cover (uniformly or in an adaptive way). These issues make this approach less useful.

Thus, we use a different approach. On each level $k = 0, \ldots, l$ we use the minimal regularization parameter β_k so that we have a different variational

form on each level, i.e., now we are faced with a sequence of nonnested discretization spaces with non-interpolatory basis functions and a sequence of non-inherited variational forms. The results of our numerical experiments with these two multilevel approaches showed that this second approach with a level-dependent regularization parameter β_k leads to iterations with smaller convergence rates ρ than the first approach. In fact the convergence rates of a multilevel $V(1,1)$-cycle with a different variational form on each level are essentially the same as we have for a respective Neumann problem ($\rho \leq 0.25$), see [28] for details.

1.4 Numerical Experiments

We apply our PUM to the model problem

$$\begin{aligned} -\Delta u &= f \text{ in } \Omega, \\ u &= g \text{ on } \partial\Omega, \end{aligned} \tag{1.14}$$

in two and three dimensions. In all our experiments we use a linear spline as the generation weight function $\mathcal{W}$ for the partition of unity (1.3) and we use uniform, quasi Monte Carlo and graded point sets P for our cover construction algorithm [13]. Here, we use $\alpha = 1.3$ so that we have an overlap of 30% of two cover patches (in the uniform case). As local approximation spaces we use Legendre polynomials.

Example 1. In our first example we consider the model problem (1.14) on the unit square $\Omega = (0,1)^2$ and choose f and g such that the solution to (1.14) is given by

$$u(x,y) = \arctan\Big(100\big(\frac{x+y}{\sqrt{2}} - 0.8\big)\big(x - x^2\big)\big(y - y^2\big)\Big), \tag{1.15}$$

see Figure 1.1.

We use the uniform h-version of our PUM for the approximation of (1.14), i.e., we use the cell centers of a uniform grid for the cover construction. Here, we increase the number of points $N = \mathrm{card}(P) = 2^{ld}$ for our PUM construction by increasing the refinement level l of the underlying uniform grid. Hence, we expect an algebraic error estimate of the form

$$\|u - u_l^{\mathrm{PU}}\| = O(\mathsf{dof}_l^{\rho})$$

and compute the respective convergence rates

$$\rho := \frac{\log\Big(\frac{\|u-u_l^{\mathrm{PU}}\|}{\|u-u_{l-1}^{\mathrm{PU}}\|}\Big)}{\log(\frac{\mathsf{dof}_l}{\mathsf{dof}_{l-1}})} \tag{1.16}$$

Table 1.1. Relative errors e (1.17) and convergence rates ρ (1.16) for Example 1 and solution (1.15) with the uniform h-version of the PUM.

l	N	p	dof	e_{L^∞}	ρ_{L^∞}	e_{L^2}	ρ_{L^2}	e_{H^1}	ρ_{H^1}
3	64	1	192	1.554_{-1}		9.484_{-2}		3.880_{-1}	
4	256	1	768	5.059_{-2}	-0.810	2.806_{-2}	-0.879	1.997_{-1}	-0.479
5	1024	1	3072	1.444_{-2}	-0.904	7.503_{-3}	-0.951	1.003_{-1}	-0.497
6	4096	1	12288	3.969_{-3}	-0.932	1.913_{-3}	-0.986	5.028_{-2}	-0.498
7	16384	1	49152	1.020_{-3}	-0.980	4.816_{-4}	-0.995	2.515_{-2}	-0.500
8	65536	1	196608	2.567_{-4}	-0.995	1.205_{-4}	-0.999	1.258_{-2}	-0.500
9	262144	1	786432	6.423_{-5}	-0.999	3.012_{-5}	-1.000	6.287_{-3}	-0.500
10	1048576	1	3145728	1.606_{-5}	-1.000	7.529_{-6}	-1.000	3.143_{-3}	-0.500

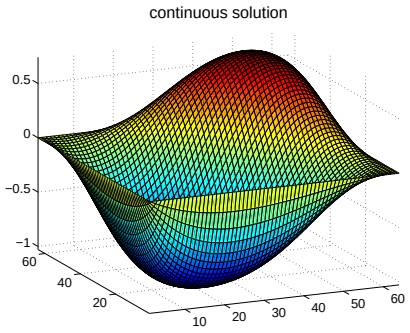

Figure 1.1. Surface plot of the solution (1.15).

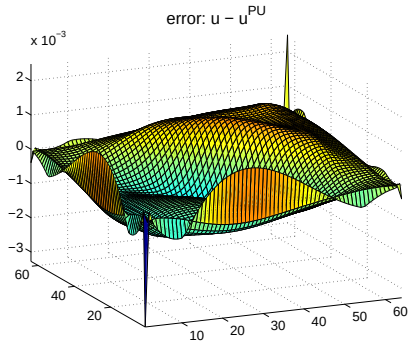

Figure 1.2. Surface plot of the error $u - u_l^{\mathrm{PU}}$ with $l = 6$ for the h-version PUM.

from the errors $u - u_l^{\mathrm{PU}}$ measured in various norms. These error norms $\|u - u_l^{\mathrm{PU}}\|$ are computed with the help of the numerical quadrature scheme presented in [13], i.e., the L^∞-norm is approximated in the quadrature points only.

Note that due to the use of such regular point sets P we have $N^{-1/d} = h$ and we can compute the standard $O(h^\gamma)$ convergence rates γ for an h-version PUM. We have $\mathsf{dof} \simeq Np^d = h^{-d}p^d$ and thus we find

$$\gamma = -\rho d.$$

Due to our choice of parameters we expect a quadratic h-convergence in the L^2-norm and a linear h-convergence in the H^1-norm, i.e., we expect to measure $\rho_{L^2} = -1$ and $\rho_{H^1} = -0.5$ in this two dimensional example. This anticipated convergence behavior can be observed from the relative errors

$$e_{L^\infty} := \frac{\|u - u_l^{\mathrm{PU}}\|_{L^\infty}}{\|u\|_{L^\infty}}, \quad e_{L^2} := \frac{\|u - u_l^{\mathrm{PU}}\|_{L^2}}{\|u\|_{L^2}}, \quad \text{and} \quad e_{H^1} := \frac{\|\nabla(u - u_l^{\mathrm{PU}})\|_{L^2}}{\|\nabla u\|_{L^2}} \tag{1.17}$$

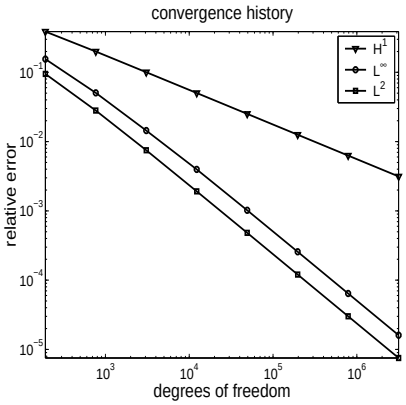

Figure 1.3. Convergence history of the h-version of the PUM for Example 1 and solution (1.15).

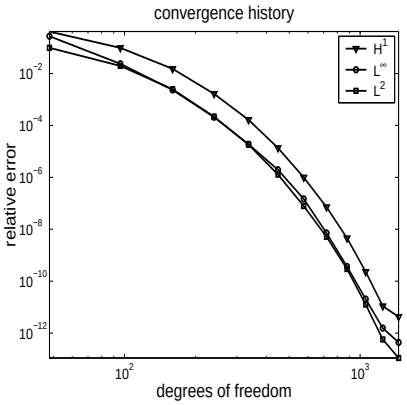

Figure 1.4. Convergence history of the p-version of the PUM for Example 1 and solution (1.18).

displayed in Table 1.1 and the respective convergence rates ρ_{L^∞}, ρ_{L^2} and ρ_{H^1}. Also the graphs depicted in Figure 1.3 clearly show the expected convergence behavior of the h-version of our PUM with linear polynomials.

Let us now consider higher order discretizations, i.e., we now use Legendre polynomials of degree $p = 1, \ldots, 12$ for the approximation of (1.14). Here, we choose f and g such that the solution is given by the analytic function

$$u(x, y) = \exp(4(x + y)). \tag{1.18}$$

Due to the unlimited smoothness of (1.18) we expect that the algebraic convergence rates (1.16) for the L^2-norm is given by $\rho_{L^2} = -\frac{p+1}{d}$ and by $\rho_{H^1} = -\frac{p}{d}$ for the energy norm if we use an h-refinement. This anticipated convergence behavior can be observed from the numbers displayed in Table 1.2. We see some fluctuations in the convergence rates for higher polynomial degrees ($p > 7$) where we do not fully achieve the anticipated convergence rates. Here, the errors are already so small ($\|e\|_{L^\infty} \leq 10^{-12}$) that we experience some effects from the limited accuracy of floating-point arithmetic. If we use a p-refinement where we increase the polynomial degree successively but keep the number of points fixed we anticipate an exponential convergence behavior. From the plots of the relative errors against the number of degrees of freedom given in Figure 1.4, we can observed the exponential convergence of the p-version of our PUM for smooth functions as expected. Again, we see a drop-off in the convergence rates for very small errors ($\|e\|_{L^\infty} \leq 10^{-12}$).

In summary, the results of this example clearly show that the implementation of Dirichlet boundary conditions by Nitsche's method preserves the approximation properties of the h-version as well as the p-version of our PUM.

Table 1.2. Relative errors e (1.17) and convergence rates ρ (1.16) for Example 1 and solution (1.18) with the p-version of the PUM.

l	N	p	dof	e_{L^∞}	ρ_{L^∞}	e_{L^2}	ρ_{L^2}	e_{H^1}	ρ_{H^1}
1	4	2	24	1.069_{-1}	-0.808	1.287_{-1}	-0.974	3.045_{-1}	-0.536
2	16	2	96	2.373_{-2}	-1.086	1.979_{-2}	-1.350	9.773_{-2}	-0.820
3	64	2	384	4.324_{-3}	-1.228	2.196_{-3}	-1.586	2.530_{-2}	-0.975
4	256	2	1536	6.411_{-4}	-1.377	2.398_{-4}	-1.597	6.258_{-3}	-1.008
1	4	3	40	1.991_{-2}	-1.233	3.235_{-2}	-1.856	9.496_{-2}	-1.097
2	16	3	160	2.348_{-3}	-1.542	2.474_{-3}	-1.855	1.522_{-2}	-1.321
3	64	3	640	2.257_{-4}	-1.689	1.532_{-4}	-2.007	2.000_{-3}	-1.464
4	256	3	2560	1.824_{-5}	-1.815	8.843_{-6}	-2.057	2.455_{-4}	-1.513
1	4	4	60	3.584_{-3}	-1.675	5.667_{-3}	-2.255	2.096_{-2}	-1.586
2	16	4	240	2.095_{-4}	-2.048	2.169_{-4}	-2.354	1.656_{-3}	-1.831
3	64	4	960	9.712_{-6}	-2.216	6.193_{-6}	-2.565	1.004_{-4}	-2.022
4	256	4	3840	3.881_{-7}	-2.323	1.661_{-7}	-2.610	5.781_{-6}	-2.059
1	4	5	84	8.455_{-4}	-1.884	7.812_{-4}	-2.691	3.706_{-3}	-2.042
2	16	5	336	1.878_{-5}	-2.746	1.848_{-5}	-2.701	1.658_{-4}	-2.241
3	64	5	1344	4.617_{-7}	-2.673	3.087_{-7}	-2.952	5.507_{-6}	-2.456
4	256	5	5376	9.590_{-9}	-2.795	4.724_{-9}	-3.015	1.693_{-7}	-2.512
1	4	6	112	1.158_{-4}	-2.525	1.151_{-4}	-2.960	6.213_{-4}	-2.400
2	16	6	448	1.962_{-6}	-2.942	1.282_{-6}	-3.244	1.368_{-5}	-2.753
3	64	6	1792	2.278_{-8}	-3.214	1.124_{-8}	-3.417	2.385_{-7}	-2.921
4	256	6	7168	2.117_{-10}	-3.375	9.043_{-11}	-3.479	3.851_{-9}	-2.976
1	4	7	144	1.739_{-5}	-2.745	1.397_{-5}	-3.452	8.879_{-5}	-2.858
2	16	7	576	1.483_{-7}	-3.436	7.875_{-8}	-3.736	1.000_{-6}	-3.236
3	64	7	2304	8.300_{-10}	-3.741	3.393_{-10}	-3.929	8.690_{-9}	-3.423
4	256	7	9216	4.167_{-12}	-3.819	1.303_{-12}	-4.012	6.865_{-11}	-3.492
1	4	8	180	1.594_{-6}	-3.385	1.731_{-6}	-3.790	1.206_{-5}	-3.234
2	16	8	720	7.233_{-9}	-3.892	5.162_{-9}	-4.195	7.233_{-8}	-3.691
3	64	8	2880	2.378_{-11}	-4.124	1.215_{-11}	-4.365	3.372_{-10}	-3.872
4	256	8	11520	1.155_{-13}	-3.843	4.033_{-14}	-4.117	2.044_{-12}	-3.683
1	4	9	220	1.558_{-7}	-3.848	1.886_{-7}	-4.180	1.439_{-6}	-3.638
2	16	9	880	3.698_{-10}	-4.359	2.963_{-10}	-4.657	4.577_{-9}	-4.148
3	64	9	3520	1.052_{-12}	-4.229	8.197_{-13}	-4.249	2.898_{-11}	-3.652
1	4	10	264	1.747_{-8}	-4.498	1.705_{-8}	-4.516	1.482_{-7}	-4.070
2	16	10	1056	2.048_{-11}	-4.868	1.263_{-11}	-5.199	2.315_{-10}	-4.661
3	64	10	4224	9.127_{-14}	-3.905	2.960_{-14}	-4.369	1.197_{-12}	-3.798
1	4	11	312	1.963_{-9}	-4.788	1.479_{-9}	-4.991	1.408_{-8}	-4.541
2	16	11	1248	1.562_{-12}	-5.148	5.720_{-13}	-5.668	1.107_{-11}	-5.156
1	4	12	364	1.793_{-10}	-5.003	1.226_{-10}	-5.420	1.273_{-9}	-4.908
2	16	12	1456	4.401_{-13}	-4.335	1.107_{-13}	-5.057	4.271_{-12}	-4.110

Example 2. In our second example we consider the model problem (1.14) on the unit cube $\Omega = (0,1)^3$ where we choose f and g such that the solution to (1.14) is given by

$$u(x) = \|x\|_2^5. \tag{1.19}$$

Table 1.3. Relative errors e (1.17) and convergence rates ρ (1.16) for Example 2 with the uniform h-version of the PUM.

l	N	p	dof	e_{L^∞}	ρ_{L^∞}	e_{L^2}	ρ_{L^2}	e_{H^1}	ρ_{H^1}
1	8	1	32	2.054_{-1}	-0.450	1.349_{-1}	-0.617	4.967_{-1}	-0.189
2	64	1	256	8.970_{-2}	-0.398	3.239_{-2}	-0.686	2.537_{-1}	-0.323
3	512	1	2048	2.448_{-2}	-0.625	9.225_{-3}	-0.604	1.303_{-1}	-0.321
4	4096	1	16384	5.974_{-3}	-0.678	2.640_{-3}	-0.602	6.565_{-2}	-0.330
5	32768	1	131072	1.573_{-3}	-0.642	7.183_{-4}	-0.626	3.286_{-2}	-0.333
6	262144	1	1048576	3.872_{-4}	-0.674	1.886_{-4}	-0.643	1.643_{-2}	-0.333
7	2097152	1	8388608	9.616_{-5}	-0.670	4.836_{-5}	-0.654	8.213_{-3}	-0.333

Table 1.4. Relative errors e (1.17) and convergence rates ρ (1.16) for Example 2 with the h-version of the PUM using Halton$(2, 3, 5)$ point sets.

l	N	p	dof	e_{L^∞}	ρ_{L^∞}	e_{L^2}	ρ_{L^2}	e_{H^1}	ρ_{H^1}
2	64	1	256	2.676_{-2}	-0.653	1.034_{-2}	-0.824	2.000_{-1}	-0.290
4	176	1	704	1.999_{-2}	-0.288	9.083_{-3}	-0.128	1.832_{-1}	-0.087
6	1373	1	5492	5.142_{-3}	-0.661	2.724_{-3}	-0.586	9.289_{-2}	-0.331
6	10606	1	42424	1.621_{-3}	-0.565	7.277_{-4}	-0.646	4.686_{-2}	-0.335
7	91820	1	367280	3.763_{-4}	-0.676	1.847_{-4}	-0.635	2.322_{-2}	-0.325

Again, we begin with a uniformly refined sequence of point sets before we discuss the results of the h-version of our PUM based on randomly chosen points. We expect to measure convergence rates $\rho_{L^2} = -\frac{2}{3}$ and $\rho_{H^1} = -\frac{1}{3}$ which correspond to the usual $O(h^2)$ and $O(h)$ behavior in three dimensions. The measured errors and convergence rates for the uniform h-version of our PUM are given in Table 1.3. From these we can clearly observe the anticipated convergence behavior.

Up to now we have considered uniform point sets only to avoid any fluctuations in the measured convergence rates due to an irregular point distribution. Now that we have seen that our PUM does indeed converge with the expected properties we turn to the use of general point sets. To this end, we employ a Halton$(2, 3, 5)$ sequence[1] to generate an initial point set for our tree-based cover construction algorithm [13]. Here, we use the same number of points as we had for the uniform point set (see N in Table 1.3) but since our cover construction automatically introduces additional points to insure the shape regularity of the cover patches ω_i we find a larger number of points N than before. Hence, the number points cannot be prescribed exactly so that N does not grow by a constant factor of 2^d from row to row in Table 1.4. The values of l now correspond to the maximal refinement level of the cover tree, i.e., the minimal support size is given by $\operatorname{diam}(\omega_i) \simeq \alpha 2^{-l}$. This

[1] Halton sequences are quasi Monte Carlo sequences, which are used in sampling and numerical integration. Consider $n \in \mathbb{N}_0$ given as $\sum_j n_j p^j = n$ for some prime p. We can define the transformation H_p from $\mathbb{N}_0$ to $[0, 1]$ with $n \mapsto H_p(n) = \sum_j n_j p^{-j-1}$. Then, the Halton$(p, q)$ sequence with N points in two dimensions is given by $\{(H_p(n), H_q(n)) \,|\, n = 0, \ldots, N-1\}$.

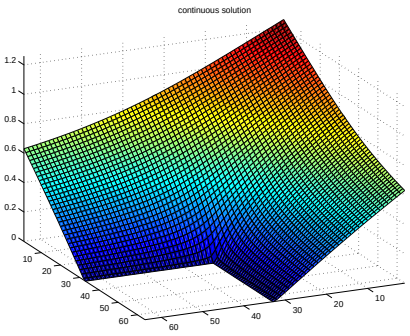

Figure 1.5. Surface plot of solution (1.20) for Example 3.

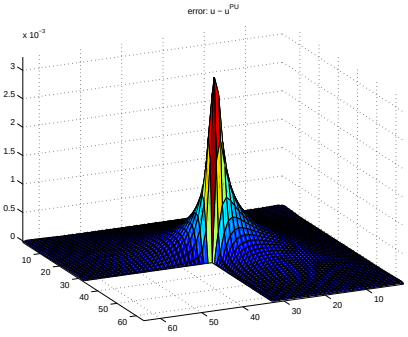

Figure 1.6. Error $u - u_l^{\mathrm{PU}}$ with $l = 6$ for Example 3.

Table 1.5. Relative errors e (1.17) and convergence rates ρ (1.16) for Example 3 with the uniform h-version of the PUM.

l	N	p	dof	e_{L^∞}	ρ_{L^∞}	e_{L^2}	ρ_{L^2}	e_{H^1}	ρ_{H^1}
3	48	1	144	5.792_{-2}		6.487_{-3}		1.112_{-1}	
4	192	1	576	3.122_{-2}	-0.446	3.195_{-3}	-0.511	7.296_{-2}	-0.304
5	768	1	2304	1.816_{-2}	-0.391	1.434_{-3}	-0.578	4.723_{-2}	-0.314
6	3072	1	9216	1.160_{-2}	-0.324	5.659_{-4}	-0.671	3.003_{-2}	-0.327
7	12288	1	36864	7.275_{-3}	-0.336	2.272_{-4}	-0.658	1.906_{-2}	-0.328
8	49152	1	147456	4.507_{-3}	-0.345	9.244_{-5}	-0.649	1.208_{-2}	-0.329
9	196608	1	589824	2.869_{-3}	-0.326	3.629_{-5}	-0.674	7.622_{-3}	-0.332
10	786432	1	2359296	1.826_{-3}	-0.326	1.424_{-5}	-0.675	4.804_{-3}	-0.333

fluctuation in the number of degrees of freedom, however, should not effect the measured convergence rates substantially since the Halton point sets are uniformly distributed. The results presented in Table 1.4 clearly support this assertion. Again, we find $\rho_{L^2} = -\frac{2}{3}$ and $\rho_{H^1} = -\frac{1}{3}$.

Example 3. So far all considered problems were H^2-regular and hence the solutions of these problems could be approximated with the usual optimal convergence rates ρ. Let us now turn to the treatment of problems with singular solutions. To this end, we consider our model problem (1.14) on an L-shaped domain $\Omega = (-1,1)^2 \setminus [0,1)^2$ where we choose f and g such that the solution (see Figure 1.5) is given by

$$u(r,\theta) = r^{\frac{2}{3}} \sin\left(\frac{2\theta - \pi}{3}\right) \tag{1.20}$$

which is in H^s with $s < 1 + \frac{2}{3}$ only. Hence, we cannot expect to measure the same convergence rates as we did in the previous examples. From finite element theory [31, Chapter 8] we know that a solution u to a homogeneous Dirichlet problem on an L-shaped domain can be split into a regular part $u_R \in H^2$ and a singular part u_S where this singular part is given by the our solution

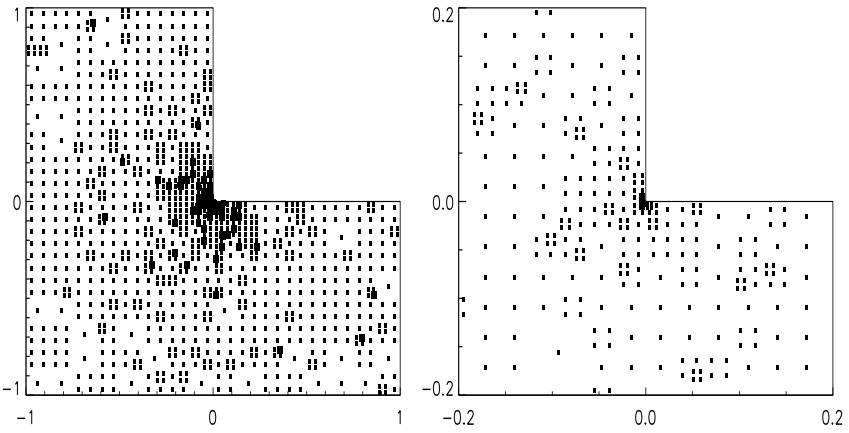

Figure 1.7. Fine level point set P_{10} generated from a graded Halton$(2,3)$ point set with 1024 points (left), zoom-in (right).

(1.20). Hence, this example represents the hard part of the general situation. If we can approximate solution (1.20) with a particular convergence rate then we can approximate any solution to a homogeneous Dirichlet problem on an L-shaped domain using the same PUM space with the same convergence rate.

It is well-known that a uniform h-version with linear elements will give an $O(h^{2/3})$ convergence in the energy norm only. Thus, we may achieve a convergence of $\rho_{H^1} < -\frac{1}{3}$ with the corresponding linear h-version PUM where we approximate the (singular) boundary value by Nitsche's method. This anticipated convergence behavior can be observed from the measured errors (see also Figure 1.9 (left)) and convergence rates displayed in Table 1.5. From the surface plot of the continuous solution (1.20) given in Figure 1.5 and the surface plot of the error $u - u_l^{\mathrm{PU}}$ with $l = 6$ depicted in Figure 1.6 we see the singular character of the solution at the re-entrant corner.

One approach to this singular problem is the use of an adaptive h-version PUM so that the singularity is resolved. To this end we use a graded Halton$(2,3)$ point set, see Figure 1.7, for the cover construction. The results of this experiment are given in Table 1.6 and Figure 1.9 (center). The measured convergence rates clearly indicate that we can resolve the singularity at the re-entrant corner by local (h-type) refinement of the cover patches. Again, we measure the optimal rates $\rho_{L^2} = -1$ and $\rho_{H^1} = -\frac{1}{2}$.

The PUM approach, however, also allows for a different p-type adaptation process. One benefit of the PUM approach is the independence of the local approximation spaces, i.e., we may include singular functions in a local approximation space without the need to pay any attention to neighboring (overlapping) local spaces. Hence, the introduction of a singular function into the local approximation spaces $V_i^{p_i}$ in the vicinity of the re-entrant corner can be realized very easily within the PUM. From finite element theory we know

Table 1.6. Relative errors e (1.17) and convergence rates ρ (1.16) for Example 3 with the h-version of the PUM using graded Halton$(2,3)$ point sets.

l	N	p	dof	e_{L^∞}	ρ_{L^∞}	e_{L^2}	ρ_{L^2}	e_{H^1}	ρ_{H^1}
5	186	1	558	8.075_{-2}	-0.398	2.896_{-2}	-0.560	1.877_{-1}	-0.265
7	300	1	900	2.727_{-2}	-2.271	1.059_{-2}	-2.104	1.261_{-1}	-0.833
10	1293	1	3879	7.265_{-3}	-0.905	3.173_{-3}	-0.825	6.569_{-2}	-0.446
11	4968	1	14904	1.945_{-3}	-0.979	7.927_{-4}	-1.030	3.268_{-2}	-0.519
14	20142	1	60426	5.029_{-4}	-0.966	2.048_{-4}	-0.967	1.677_{-2}	-0.476
17	80574	1	241722	1.394_{-4}	-0.925	5.030_{-5}	-1.013	8.239_{-3}	-0.513
17	317637	1	952911	3.820_{-5}	-0.944	1.272_{-5}	-1.002	4.158_{-3}	-0.499
20	1310847	1	3932541	9.223_{-6}	-1.003	3.224_{-6}	-0.969	2.092_{-3}	-0.485

that this may improve the convergence from $O(h^{2/3})$ in the energy norm to the usual $O(h)$ behavior.

To this end, consider the sub-domains $\Omega_p := \Omega \setminus [-a,a]^2 \subset \Omega$ and $\Omega_a := \Omega \cap [-a,a]^2 \subset \Omega$. On the cover patches ω_i whose associated center point x_i is sufficiently far away from the singularity at the origin, i.e. $x_i \in \Omega_p$, we use the linear Legendre polynomials as before to approximate the (smooth part of the) solution. But close to the singularity, $x_i \in \Omega_a$, we use augmented local approximation spaces $V_i^{p_i^a} := \mathrm{span}\langle V_i^{p_i}, \Phi\rangle$ where Φ is the (global) singular function (1.20). Similar constructions have also been used in the GFEM [32] and in the FEM [31] context.

The numerical results of this experiment with two different values for a, namely $a = 0.5$ and $a = 0.25$, are presented in Table 1.7 and Figure 1.9 (right). From the numbers given there we can clearly observe that the measured convergence rates are now $\rho_{L^2} = -1$ and $\rho_{H^1} = -\frac{1}{2}$ which correspond to the usual $O(h^2)$ and $O(h)$ convergence behavior respectively. This improvement in the error evolution can also be observed from a comparison of the plots depicted in Figure 1.9. The size of the sub-domain Ω_a where we use augmented local spaces $V_i^{p_i^a}$ essentially determines the location and the absolute value of the maximal error which can be observed from the surface plots given in Figure 1.8. But it has no effect on the (asymptotic) convergence rates as long as it is fixed on all levels.

Finally, we use the augmented p-version of our PUM to approximate (1.14) on the L-shaped domain where we choose f and g such that the solution is given by

$$u(r,\theta) = (1-(r\cos(\theta))^2)(1-(r\sin(\theta))^2) r^{\frac{2}{3}} \sin\Big(\frac{2\theta-\pi}{3}\Big), \tag{1.21}$$

see Figure 1.10. Again, we use augmented spaces in Ω_a with $a = 0.25$ but we now use a p-version refinement. Note that we use the singular function (1.20) as before for the augmentation of the local spaces, we do not use the solution (1.21). Since the introduction of the singularity into the PUM space V^{PU} should resolve the singularity at the re-entrant corner, we expect

Table 1.7. Relative errors e (1.17) and convergence rates ρ (1.16) for Example 3 with the uniform h-version of the PUM using augmented local spaces.

l	N	p	dof	e_{L^∞}	ρ_{L^∞}	e_{L^2}	ρ_{L^2}	e_{H^1}	ρ_{H^1}
				$a = 0.5$					
2	12	1	39	2.186_{-2}		8.939_{-3}		8.802_{-2}	
3	48	1	156	5.897_{-3}	-0.945	2.141_{-3}	-1.031	4.044_{-2}	-0.561
4	192	1	624	1.727_{-3}	-0.886	5.182_{-4}	-1.023	1.925_{-2}	-0.535
5	768	1	2496	4.896_{-4}	-0.909	1.284_{-4}	-1.006	9.330_{-3}	-0.523
6	3072	1	9984	1.278_{-4}	-0.969	3.204_{-5}	-1.002	4.559_{-3}	-0.517
7	12288	1	39936	3.310_{-5}	-0.974	8.035_{-6}	-0.998	2.256_{-3}	-0.508
8	49152	1	159744	8.483_{-6}	-0.982	2.014_{-6}	-0.998	1.122_{-3}	-0.504
9	196608	1	638976	2.122_{-6}	-1.000	5.043_{-7}	-0.999	5.594_{-4}	-0.502
				$a = 0.25$					
2	12	1	39	2.186_{-2}		8.939_{-3}		8.802_{-2}	
3	48	1	147	1.054_{-2}	-0.550	4.121_{-3}	-0.584	6.207_{-2}	-0.263
4	192	1	588	3.635_{-3}	-0.768	1.043_{-3}	-0.991	3.066_{-2}	-0.509
5	768	1	2352	1.117_{-3}	-0.851	2.511_{-4}	-1.027	1.497_{-2}	-0.517
6	3072	1	9408	3.053_{-4}	-0.936	6.051_{-5}	-1.027	7.335_{-3}	-0.515
7	12288	1	37632	8.095_{-5}	-0.957	1.486_{-5}	-1.013	3.630_{-3}	-0.507
8	49152	1	150528	2.102_{-5}	-0.973	3.683_{-6}	-1.006	1.805_{-3}	-0.504
9	196608	1	602112	5.305_{-6}	-0.993	9.169_{-7}	-1.003	8.999_{-4}	-0.502

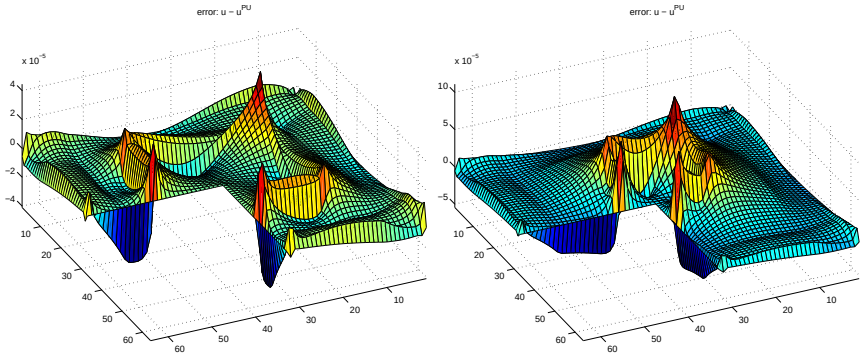

Figure 1.8. Error $u - u_l^{\mathrm{PU}}$ with $l = 6$ for the h-version PUM with augmented local spaces (left: $a = 0.5$, right: $a = 0.25$).

an exponential convergence of the p-version for the singular solution (1.21). This anticipated convergence behavior can be observed from the plots given in Figure 1.14 for larger errors ($\|e\|_{L^\infty} \geq 10^{-4}$). Then, we experience some pollution effect within Ω_a which comes from the couplings between overlapping polynomial spaces in Ω_p and augmented spaces in Ω_a, see Figures 1.11, 1.12, and 1.13. Here, a smaller overlap between augmented and polynomial spaces may overcome this pollution effect and could extend the exponential convergence behavior even further. Nonetheless, we are able to approximate

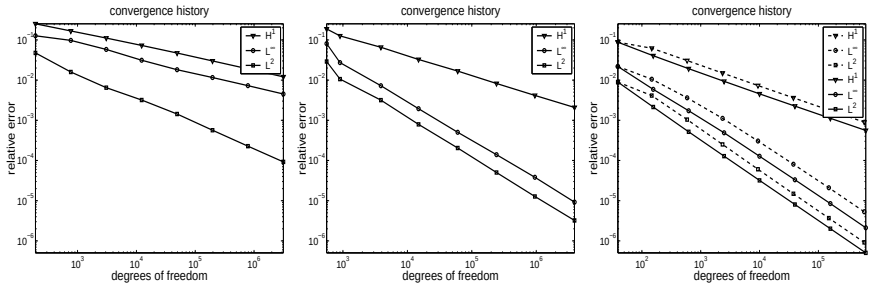

Figure 1.9. Convergence history of the h-version of the PUM with linear local spaces (left: uniform point set, center: graded Halton$(2, 3)$ point set) and augmented local spaces (right: solid lines $a = 0.5$, dashed lines $a = 0.25$) for Example 3.

the singular solution (1.21) with a relative accuracy of five digits with about 1000 degrees of freedom only.

In summary, the results of our numerical experiments clearly show the expected convergence properties of our PUM independent of the boundary conditions. The implementation of Dirichlet boundary conditions by Nitsche's method has no adverse effect on the convergence rates for regular as well as singular solutions. We achieve the optimal convergence rates for regular as well as irregular point sets, polynomial basis functions and singular basis functions.

1.5 Concluding Remarks

We presented a meshfree Galerkin discretization technique, the partition of unity method, for the numerical treatment of elliptic partial differential equations of second order. We focused on the implementation of Dirichlet boundary conditions which is not trivial since the shape functions are non-interpolatory. Here, an almost forgotten method due to Nitsche enabled us to use our partition of unity shape functions without any modification for the treatment of Dirichlet problems.

This approach involves only the original partition of unity space and the evaluation of an additional boundary integral term so that there is no need to change the method or the implementation in any way. We can use our general cover construction algorithm [13], our sparse grid integration scheme [13] as well as our multilevel solver [14] without any modification for the treatment of Dirichlet problems with our partition of unity method. Hence, also the parallelization and parallel efficiency of the method [15] is not effected by the boundary conditions. Furthermore, Nitsche's method is also applicable to general domains, it was in fact developed for general domains.

The results of our numerical experiments where we considered two- and three-dimensional problems with several million degrees of freedom clearly

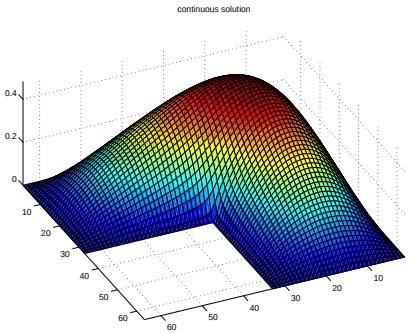

Figure 1.10. Surface plot of solution (1.21) for Example 3.

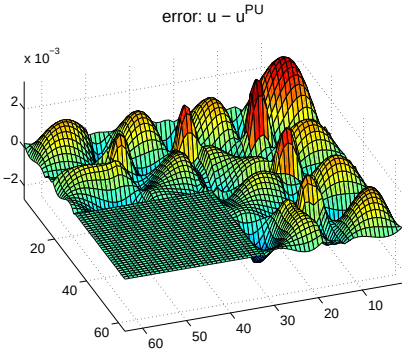

Figure 1.11. Error $u - u_l^{\mathrm{PU}}$ with $l = 2$, $p = 3$ for Example 3.

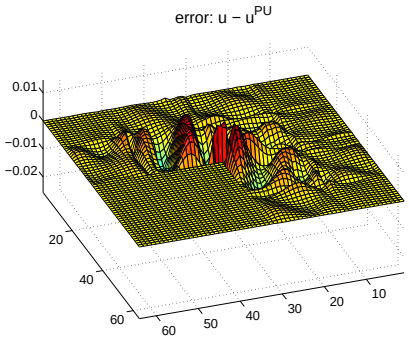

Figure 1.12. Error $u - u_l^{\mathrm{PU}}$ with $l = 2$, $p = 5$ for Example 3.

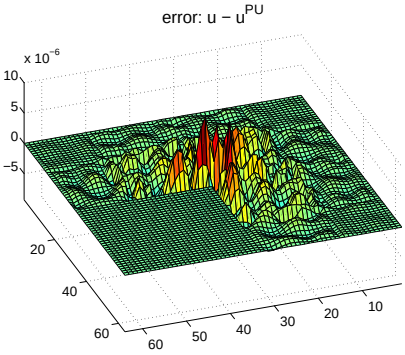

Figure 1.13. Error $u - u_l^{\mathrm{PU}}$ with $l = 2$, $p = 8$ for Example 3.

showed that we achieve optimal convergence rates of the h-version and p-version of our PUM for Dirichlet problems. This observation holds not only for regular point sets and regular solutions but also for highly adaptive discretizations and singular solutions.

References

1. D. N. Arnold, F. Brezzi, B. Cockburn, and D. Marini, *Discontinuous Galerkin Methods for Elliptic Problems*, in Discontinuous Galerkin Methods: Theory, Computation and Applications, B. Cockburn, G. Karniadakis, and C.-W. Shu, eds., Springer, 1999, pp. 89–101.
2. I. Babuška, *Numerical Solution of Boundary Value Problems by the Perturbated Variational Principle*, Tech. Note BN-624, University of Maryland, 1969.
3. ———, *The Finite Element Method with Lagrangian Multipliers*, Numer. Math., 20 (1973), pp. 179–192.

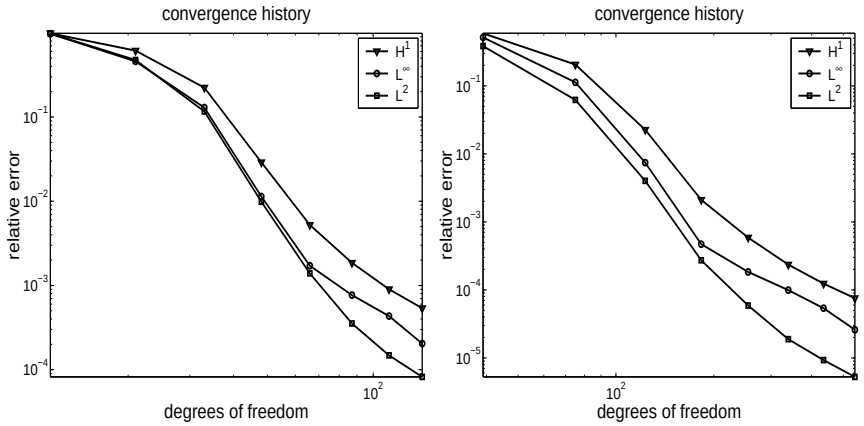

Figure 1.14. Convergence history of the augmented p-version of the PUM with linear local spaces $l = 1$ (left) and $l = 2$ (right) for Example 3 with solution (1.21).

4. I. Babuška, U. Banerjee, and J. E. Osborn, *Meshless and Generalized Finite Element Methods: A Survey of Some Major Results*, in Meshfree Methods for Partial Differential Equations, M. Griebel and M. A. Schweitzer, eds., Lecture Notes in Computational Science and Engineering, Springer, 2002.
5. I. Babuška and J. M. Melenk, *The Partition of Unity Finite Element Method: Basic Theory and Applications*, Comput. Meth. Appl. Mech. Engrg., 139 (1996), pp. 289–314. Special Issue on Meshless Methods.
6. ———, *The Partition of Unity Method*, Int. J. Numer. Meth. Engrg., 40 (1997), pp. 727–758.
7. W. W. Bradburry and R. Fletcher, *New Iterative Methods for the Solution of the Eigenproblem*, Numer. Math., 9 (1966), pp. 259–267.
8. J. H. Bramble, *The Lagrange Multiplier Method for Dirichlet's Problem*, Math. Comp., 37 (1981), pp. 1–11.
9. F. Brezzi, L. P. Franca, D. Marini, and A. Russo, *Stabilization Techniques for Domain Decomposition Methods with Non-matching Grids*, in Domain Decomposition Methods in Science and Engineering, P. E. Bjørstad, M. S. Espedal, and D. E. Keyes, eds., Domain Decomposition Press, 1998, pp. 1–11.
10. C. A. M. Duarte and J. T. Oden, *hp Clouds – A Meshless Method to Solve Boundary Value Problems*, Numer. Meth. for PDE, 12 (1996), pp. 673–705.
11. J. Garcke, *Berechnung von Eigenwerten der stationären Schrödingergleichung mit der Kombinationstechnik*, Diplomarbeit, Institut für Angewandte Mathematik, Universität Bonn, 1998.
12. M. Griebel and M. A. Schweitzer, *A Particle-Partition of Unity Method for the Solution of Elliptic, Parabolic and Hyperbolic PDE*, SIAM J. Sci. Comput., 22 (2000), pp. 853–890.
13. ———, *A Particle-Partition of Unity Method—Part II: Efficient Cover Construction and Reliable Integration*, SIAM J. Sci. Comput., 23 (2002), pp. 1655–1682.
14. ———, *A Particle-Partition of Unity Method—Part III: A Multilevel Solver*, SIAM J. Sci. Comput., (2002). to appear.

15. ———, *A Particle-Partition of Unity Method—Part IV: Parallelization*, in Meshfree Methods for Partial Differential Equations, M. Griebel and M. A. Schweitzer, eds., Lecture Notes in Computational Science and Engineering, Springer, 2002.
16. F. C. Günther and W. K. Liu, *Implementation of Boundary Conditions for Meshless Methods*, Comput. Meth. Appl. Mech. Engrg., 163 (1998), pp. 205–230.
17. W. Han and X. Meng, *Some Studies of the Reproducing Kernel Particle Method*, in Meshfree Methods for Partial Differential Equations, M. Griebel and M. A. Schweitzer, eds., Lecture Notes in Computational Science and Engineering, Springer, 2002.
18. B. Heinrich and K. Pietsch, *Nitsche Type Mortaring for some Elliptic Problems with Corner Singularities*, Tech. Rep. SFB393/00-34, Sonderforschungsbereich 393, 2000.
19. Y. Krongauz and T. Belytschko, *Enforcement of Essential Boundary Conditions in Meshless Approximations using Finite Elements*, Comput. Meth. Appl. Mech. Engrg., 131 (1996), pp. 133–145.
20. A. Kunoth, *Multilevel Preconditioning – Appending Boundary Conditions by Lagrange Multipliers*, Adv. Comput. Math., 4 (1995), pp. 145–170. Special Issue on Multiscale Methods.
21. D. E. Longsine and S. F. McCormick, *Simultaneous Rayleigh-Quotient Minimization Methods for $Ax = \lambda Bx$*, Lin. Alg. Appl., 34 (1980), pp. 195–234.
22. Y. Y. Lu, T. Belytschko, and L. Gu, *A New Implementation of the Element Free Galerkin Method*, Comput. Math. Appl. Mech. Engrg., 113 (1994), pp. 397–414.
23. J. Nitsche, *Über ein Variationsprinzip zur Lösung von Dirichlet-Problemen bei Verwendung von Teilräumen, die keinen Randbedingungen unterworfen sind*, Abh. Math. Sem. Univ. Hamburg, 36 (1970–1971), pp. 9–15.
24. J. Pitkäranta, *Boundary Subspaces for the Finite Element Method with Lagrange Multipliers*, Numer. Math., 33 (1979), pp. 273–289.
25. ———, *Local Satbility Conditions for the Babuška Method of Lagrange Multipliers*, Math. Comp., 35 (1980), pp. 1113–1129.
26. ———, *The Finite Element Method with Lagrange Multipliers for Domains with Corners*, Math. Comp., 37 (1981), pp. 13–30.
27. M. A. Schweitzer, *Ein Partikel–Galerkin–Verfahren mit Ansatzfunktionen der Partition of Unity Method*, Diplomarbeit, Institut für Angewandte Mathematik, Universität Bonn, 1997.
28. ———, *A Parallel Multilevel Partition of Unity Method*, Dissertation, Institut für Angewandte Mathematik, Universität Bonn, 2002.
29. R. Stenberg, *On some Techniques for Approximating Boundary Conditions in the Finite Element Method*, J. Comput. Appl. Math., 63 (1995), pp. 139–148.
30. ———, *Mortaring by a Method of J. A. Nitsche*, in Computational Mechanics, New Trends and Applications, S. Idelsohn, E. Onate, and E. Dvorkin, eds., 1998, pp. 1–6.
31. G. Strang and G. J. Fix, *An Analysis of the Finite Element Method*, Prentice–Hall, 1973.
32. T. Strouboulis, I. Babuška, and K. Copps, *The Design and Analysis of the Generalized Finite Element Method*, Comput. Meth. Appl. Mech. Engrg., 181 (1998), pp. 43–69.